Official journal of the American Society of Gene & Cell Therapy

MTOpen

original article

Syndecan 4 Mediates Nrf2-dependent Expansion of Bronchiolar Progenitors That Protect Against Lung Inflammation

Arif Santoso[1], Toshiaki Kikuchi[1,2], Naoki Tode[3], Taizou Hirano[1], Riyo Komatsu[1], Triya Damayanti[1], Hozumi Motohashi[4], Masayuki Yamamoto[5], Tetsuhito Kojima[6], Toshimitsu Uede[7], Toshihiro Nukiwa[1] and Masakazu Ichinose[1,3]

[1]Department of Respiratory Medicine, Tohoku University Graduate School of Medicine, Sendai, Japan; [2]Department of Respiratory Medicine and Infectious Diseases, Niigata University Graduate School of Medical and Dental Sciences, Niigata, Japan; [3]Department of Respiratory Medicine, Tohoku University Hospital, Sendai, Japan; [4]Department of Gene Expression Regulation, Institute of Development, Aging and Cancer, Tohoku University, Sendai, Japan; [5]Department of Medical Biochemistry, Tohoku University Graduate School of Medicine, Sendai, Japan; [6]Department of Pathophysiological Laboratory Sciences, Nagoya University Graduate School of Medicine, Nagoya, Japan; [7]Division of Molecular Immunology, Institute for Genetic Medicine, Hokkaido University, Sapporo, Japan

The use of lung progenitors for regenerative medicine appears promising, but their biology is not fully understood. Here, we found anti-inflammatory attributes in bronchiolar progenitors that were sorted as a multipotent subset of mouse club cells and found to express secretory leukocyte protease inhibitor (SLPI). Notably, the impaired expression of SLPI in mice increased the number of bronchiolar progenitors and decreased the lung inflammation. We determined a transcriptional profile for the bronchiolar progenitors of *Slpi*-deficient mice and identified syndecan 4, whose expression was markedly elevated as compared to that of wild-type mice. Systemic administration of recombinant syndecan 4 protein caused a substantial increase in the number of bronchiolar progenitors with concomitant attenuation of both airway and alveolar inflammation. The syndecan 4 administration also resulted in activation of the Keap1-Nrf2 antioxidant pathway in lung cells, which is critically involved in the therapeutic responses to the syndecan 4 treatment. Moreover, in 3D culture, the presence of syndecan 4 induced differentiated club cells to undergo Nrf2-dependent transition into bronchiolar progenitors. Our observations reveal that differentiative switches between bronchiolar progenitors and club cells are under the Nrf2-mediated control of SLPI and syndecan 4, suggesting the possibility of new therapeutic approaches in inflammatory lung diseases.

Received 7 October 2014; accepted 11 August 2015; advance online publication 22 September 2015. doi:10.1038/mt.2015.153

INTRODUCTION

In an attempt to develop regenerative medicine for lung diseases, considerable progress has been made in understanding lung stem/progenitor biology.[1–9] Because small airways called bronchioles are commonly injured in a variety of inflammatory clinical settings, particular attention has been paid to the regional stem/progenitor cell populations mediating epithelial homeostasis.[2,7,10–14] The bronchiolar epithelium comprises a diverse population of stem/progenitor cells and differentiated cells.[1,3,5,9] Although it has not yet been fully characterized, a subset of club cells (formerly known as Clara cells) are best understood as bronchiolar progenitors that self-renew over the long term and that can differentiate into more differentiated club cells and ciliated cells.[1–9] The bronchiolar progenitors are distinct from differentiated club cells (hereafter referred to simply as club cells, unless otherwise indicated) and characteristically express the alveolar type 2 cell marker, prosurfactant protein C (proSP-C), with lower levels of club cell secretory protein (CCSP)/Scgb1a1.[13–15] There are also functional differences between them; while club cells can be depleted by naphthalene because of the abundance of cytochrome P450 enzyme Cyp2f2, bronchiolar progenitors are resistant to naphthalene-induced depletion because of defects in the enzyme.[8,9,16,17] Naphthalene-resistant epithelial cells in the bronchioalveolar duct junction of the mouse lung are particularly proposed as putative bronchioalveolar stem cells.[9]

In addition to the functional aspects as progenitors, the CCSP-positive cells (*i.e.*, club cells and/or bronchiolar progenitors) have been shown to control the extent of lung inflammation by playing critical roles in barrier maintenance, secretion, and metabolism in airways.[16,17] However, the heterogeneity of CCSP-positive cells has discouraged further investigation into the cellular and molecular mechanisms involved in resolving lung inflammation.[2,7,9,16]

Here we make use of recent advances in flow cytometric sorting, which enable us to isolate bronchiolar progenitors and club cells separately from mouse lung cells, and test the hypothesis that these two subsets can be distinguished based upon their ability to modulate lung inflammation. Our data show that bronchiolar progenitors have higher potency to decrease lung inflammation than club cells. Moreover, we seek to clarify the molecular mechanisms

Correspondence: Toshiaki Kikuchi, Department of Respiratory Medicine and Infectious Diseases, Niigata University Graduate School of Medical and Dental Sciences, 1–757 Asahimachidori, Chuoku, Niigata 951–8510, Japan. E-mail: kikuchi@med.niigata-u.ac.jp

involved in bronchiolar progenitor physiology, and identify syndecan 4 as a downstream effector of secretory leukocyte protease inhibitor (SLPI). We also show that syndecan 4 has the therapeutic potential to increase the number of bronchiolar progenitors for anti-inflammatory responses, probably by facilitating dedifferentiation from club cells to bronchiolar progenitors via activation of the nuclear factor erythroid 2-related factor 2 (Nrf2)-dependent antioxidant pathway.

RESULTS

Bronchiolar progenitors ameliorate lung inflammation

To determine the relevance of bronchiolar progenitors in lung inflammation, we isolated bronchiolar progenitors from naive mice, and adoptively transferred them to naphthalene-injured mice (**Figure 1a–c**). We isolated bronchiolar progenitors and club cells from lung cells by flow cytometric cell sorting as previously reported,[13] and confirmed their distinctive features by bright-field microscopy (**Figure 1a**). Morphologically, while club cells defined by Lin^{neg} ($CD31^{neg}$ $CD34^{neg}$ $CD45^{neg}$) and Sca-1^{pos} autofluorescence $(AF)^{high}$ exhibited a round plump shape with an abundance of cytoplasmic organelles, bronchiolar progenitors defined by Lin^{neg} Sca-1^{pos} AF^{low} had a lower cytoplasmic/nucleus ratio with a concomitant reduction of cytoplasmic organelles (cytoplasmic/nucleus ratio, $P < 0.05$, **Supplementary Figure S1**). When adoptively transferred to naphthalene-injured mice, in which exposure to naphthalene leads to club cell depletion followed by lung inflammatory responses, bronchiolar progenitors reduced the inflammation compared to club cells (**Figure 1b,c**). Analysis of total and differential cell counts in bronchoalveolar lavage (BAL) fluid showed that the recipient mice of bronchiolar progenitors had significantly fewer cells in all cell counts except for eosinophils than recipient mice of club cells (bronchiolar progenitor transfer versus club cell transfer; total, $P < 0.001$; macrophages, $P < 0.001$; neutrophils, $P < 0.01$; lymphocytes, $P < 0.005$; eosinophils, $P > 0.1$; **Figure 1b**). There was no significant difference among these groups with respect to residual macrophages in lung tissues after BAL ($P > 0.05$; **Supplementary Figure S2**). Assessment of the lung histology also showed a marked decrease in cellular infiltrates in the peribronchiolar and perivascular spaces after adoptive transfer of bronchiolar progenitors compared to that of club cells (**Figure 1c** and **Supplementary Figure S3a**).

The phonotypic features of bronchiolar progenitors associated with the anti-inflammatory properties were assessed by immunofluorescent staining and immunoblotting (**Figure 1d,e**). Consistent with previous reports,[13,14] immunofluorescence analysis showed that bronchiolar progenitors revealed low and high levels of intracellular CCSP and proSP-C immunoreactivity, respectively (**Figure 1d**). In contrast, club cells had strong immunoreactivity only against CCSP, but not against pro-SPC (**Figure 1d**). These cell phenotypes were reflected in the amounts of CCSP and proSP-C assessed by immunoblotting; CCSP expression was lower in bronchiolar progenitors than in club cells, whereas proSP-C expression was found only in bronchiolar progenitors (**Figure 1e** and **Supplementary Figure S4a**). Moreover, bronchiolar progenitors, but not club cells, had detectable amounts of surfactant protein D (SP-D) and SLPI, both of which are capable of decreasing inflammation.[18,19]

Impaired SLPI expression increases number of anti-inflammatory bronchiolar progenitors

Given the key role of SLPI in stem/progenitor biology,[20] we determined the functional consequences of SLPI for the cellular population of bronchiolar progenitors (**Figure 2**). Notably, flow cytometric analysis showed a significantly increased number of Lin^{neg} Sca-1^{pos} AF^{low} bronchiolar progenitors in *Slpi*-deficient (*Slpi* KO) mice compared with wild-type (WT) mice ($P < 0.005$, **Figure 2a**). The increased number of bronchiolar progenitors in *Slpi* KO mice was significantly reduced by plasmid-mediated forced expression of SLPI, which was confirmed by the immunoblotting analysis in cytoplasmic and nuclear fractions of lung cells ($P < 0.01$, **Supplementary Figure S5**). Consistent with this flow cytometry result, we found that airway epithelial cells with the CCSP/proSP-C dual positivity, another characteristic of bronchiolar progenitors, were more marked in *Slpi* KO mice than in WT mice (**Figure 2b** and **Supplementary Figure S6a**). The functional relevance of our finding on the number of bronchiolar progenitors was determined by using two types of lung inflammation, from airway (**Figure 2c,d**) and alveolar injury (**Figure 2e,f**). Similar results were achieved in both types of lung inflammation. In the airway inflammation, analysis of naphthalene-injured lungs showed that *Slpi* KO mice had significantly fewer inflammatory cells in the total BAL cell count and peribronchiolar/perivascular infiltration than WT mice (naphthalene, *Slpi* KO versus WT, $P < 0.005$, **Figure 2c,d**; **Supplementary Figures S3b** and **S7a**). Even when injected with naphthalene five times daily, *Slpi* KO mice showed significantly lower numbers of total BAL cells than WT mice (naphthalene, WT versus *Slpi* KO, $P < 0.01$, **Supplementary Figure S8**). In the alveolar inflammation following bleomycin-mediated selective ablation of alveolar type 2 cells, *Slpi* KO mice had significantly lower numbers of BAL cells than WT mice, which reflected protection from the extensive parenchymal distortion and massive damage of the alveolar and distal airway compartments (bleomycin, *Slpi* KO versus WT, $P < 0.001$, **Figure 2e,f**; **Supplementary Figures S3c** and **S7b**). *In vivo* short hairpin RNA (shRNA)-mediated knockdown of the *Slpi* gene reduced the amounts of SLPI protein expression in lung cells by 24% (not shown), leading to similar results in the *Slpi* KO mice (**Figure 2g–j**). When injected with psh*Slpi*, WT mice displayed an increased number of bronchiolar progenitors for both the Lin^{neg} Sca-1^{pos} AF^{low} phenotype and the CCSP/proSP-C dual positivity ($P < 0.05$, **Figure 2g,h** and **Supplementary Figure S6b**). Injection with psh*Slpi*, but not control pshCtrl, in the WT mice also dampened the lung inflammatory responses following naphthalene exposure in total BAL cell counts and histological examination (naphthalene, psh*Slpi* versus pshCtrl, $P < 0.05$, **Figure 2i,j**). There were not any detectable differences in the numbers of Sca-1-positive cells outside the bronchiolar epithelium and CD31-positive cells between WT and *Slpi* KO mice, or pshCtrl- and psh*Slpi*-transfected WT mice (**Supplementary Figure S9**). Taken together, these results suggest that SLPI functioned as a negative regulator of the bronchiolar progenitor population that potentially helps attenuate lung inflammation.

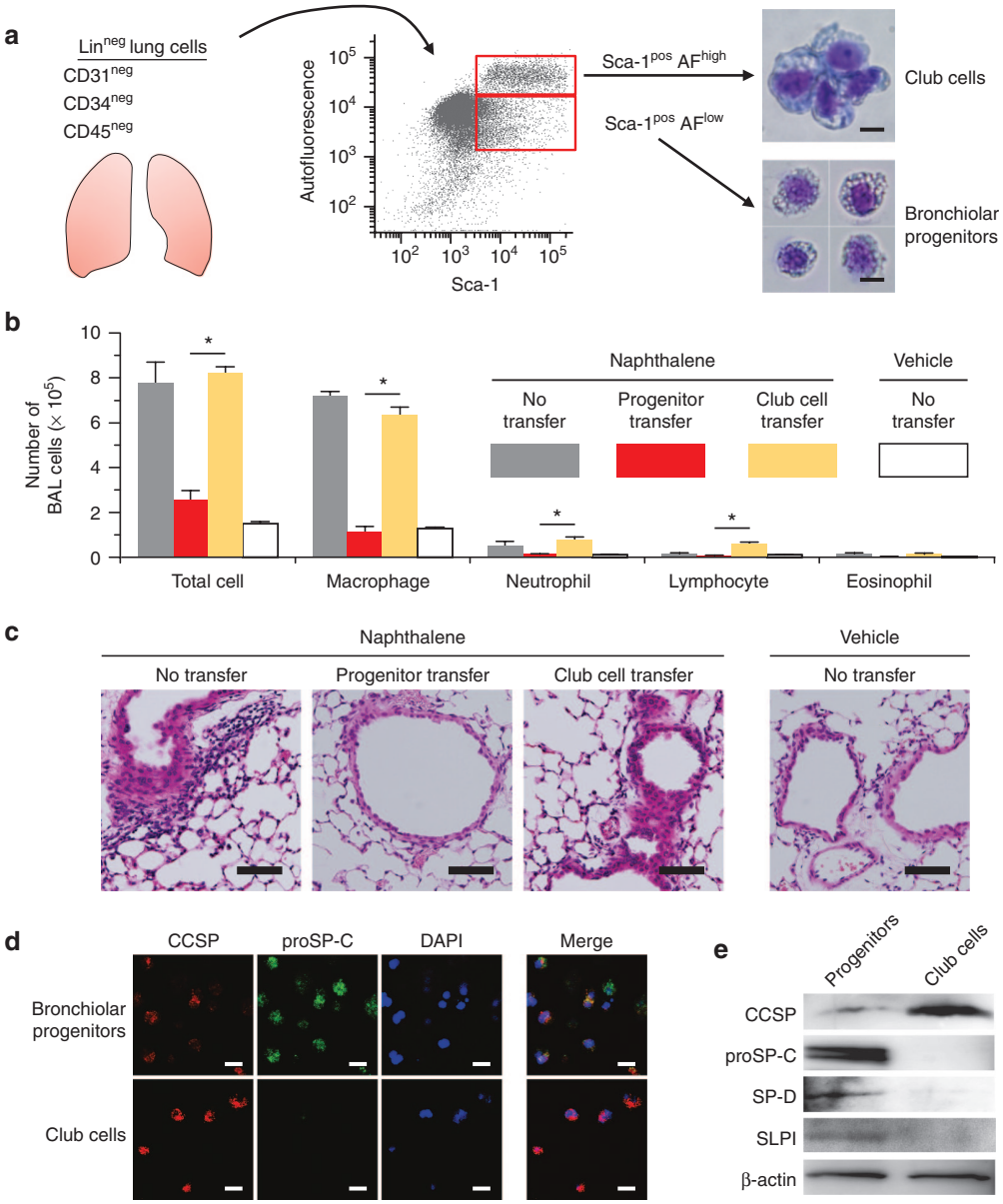

Figure 1 Anti-inflammatory effects of bronchiolar progenitors. (**a**) Isolation of bronchiolar progenitors and club cells by the phenotypic characteristics. Lineage-negative (CD31^{neg} CD34^{neg} CD45^{neg}) lung cells were fractionated into two subsets, including club cells in the Sca-1^{pos} AF^{high} gate and bronchiolar progenitors in the Sca-1^{pos} AF^{low} gate. Representative microscopic images of the Diff-Quik-stained cells are shown. Scale bar, 10 µm. (**b**,**c**) Adoptive transfer of bronchiolar progenitor and club cell subsets. C57BL/6 mice were injected intraperitoneally with naphthalene or vehicle (day 1). On day 3, the naphthalene-injected mice received intravenous injections of 10^5 bronchiolar progenitors or club cells. On day 7, the lung inflammation was assessed by total and differential counts of cells recovered in the BAL fluid (panel **b**) and histological examination of the lung sections stained with H&E (scale bar, 100 µm, panel **c**). (**d**) Club cell secretory protein (CCSP) and proSP-C staining of bronchiolar progenitors and club cells. The nuclei were identified with DAPI. Scale bar, 20 µm. (**e**) Immunoblotting of CCSP, proSP-C, SP-D, and secretory leukocyte protease inhibitor in cell lysates from bronchiolar progenitors and club cells; β-actin was used as a loading control. Asterisks indicate significant differences at 95% confidence limits. DAPI, 4′,6-diamidino-2-phenylindole, dihydrochloride; H&E, hematoxylin and eosin.

The effects caused by impaired SLPI expression are critically mediated by syndecan 4

To dissect the molecular pathway affected by the SLPI deficiency, we undertook gene expression profiling microarray of bronchiolar progenitors sorted from *Slpi* KO mice and WT mice (**Figure 3a**). The microarray data analysis revealed 71 differentially expressed genes with a greater than twofold change; 10 and 61 genes were significantly up- and downregulated, respectively, in the bronchiolar progenitors of *Slpi* KO mice compared to those of WT mice (**Supplementary Tables S1** and **S2**). Some of the genes are known to encode molecules possibly associated with stem cell/progenitor or SLPI biology, such as the genes encoding eukaryotic translation initiation factor 2 (eIF2), bone morphogenetic protein 7 (BMP7), WAP four-disulfide core domain 13 (WFDC13), and Notch1.[21–24] Of note, we found the gene encoding syndecan 4 to be most remarkably upregulated at a *P* value less than 0.0005 and a fold change of 9.1 for *Slpi* KO versus WT bronchiolar progenitors (**Figure 3a**).

Increased syndecan 4 expression in the bronchiolar progenitors of *Slpi* KO mice was confirmed by quantitative reverse

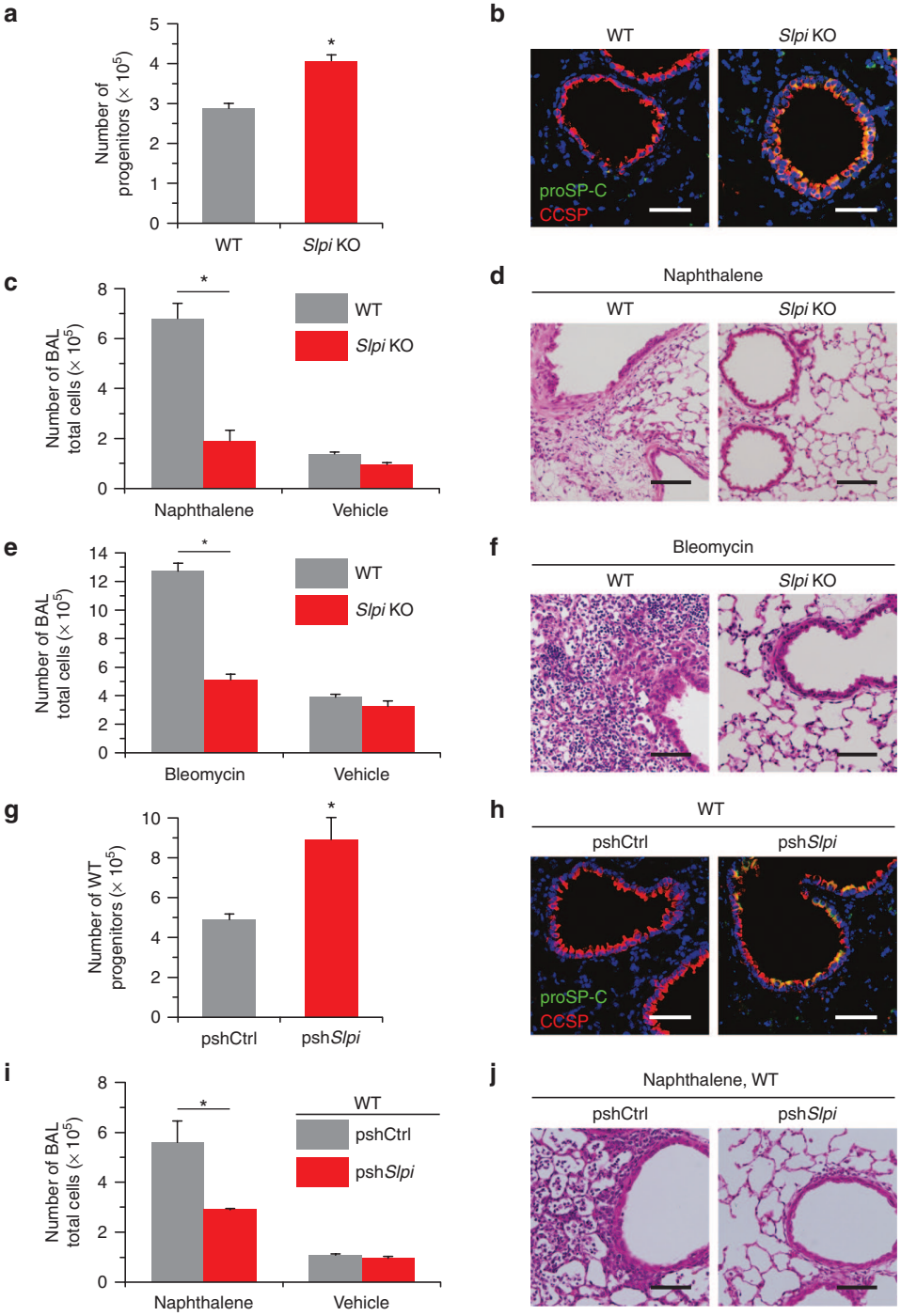

Figure 2 Impaired secretory leukocyte protease inhibitor expression increased the number of bronchiolar progenitors and decreased lung inflammation. (**a**,**b**) Increased numbers of bronchiolar progenitors in *Slpi* KO mice. Bronchiolar progenitors in WT and *Slpi* KO mice were analyzed for the phenotypic characteristics by flow cytometry (Lin^{neg} Sca-1^{pos} AF^{low}, panel **a**) and for the club cell secretory protein (CCSP)/proSP-C dual positivity by confocal microscopy (scale bar, 50 µm, panel **b**). (**c**,**d**) Naphthalene-induced inflammation in *Slpi* KO mice. WT and *Slpi* KO mice were injected intraperitoneally with naphthalene or vehicle (day 1). On day 7, the lung inflammation was assessed by total counts of cells recovered in the BAL fluid (panel **c**) and histological examination of the lung sections stained with H&E (scale bar, 100 µm, panel **d**). (**e**,**f**) Bleomycin-induced inflammation in *Slpi* KO mice. This study was similar to that in panels **c** and **d**, but the mice were injected intratracheally with bleomycin or vehicle on day 1. Scale bar, 100 µm (panel **f**). (**g**–**j**) *In vivo* transfection of a plasmid vector expressing shRNA against *Slpi* (psh*Slpi*). The study was similar to that in panels **a**–**d**, but WT mice were transfected intravenously with 50 µg of psh*Slpi* or the control vector pshCtrl on day 0. The bronchiolar progenitors in the transfected mice were analyzed by flow cytometry (Lin^{neg} Sca-1^{pos} AF^{low} cells, panel **g**) and confocal microscopy (scale bar, 50 µm, panel **h**) on day 7. To assess the lung inflammation on day 7, the transfected mice were injected with naphthalene or vehicle on day 1 (panel **i**; scale bar, 100 µm, panel **j**). For panels **a**, **c**, **e**, **g**, and **i**, data are reported as the mean ± standard error of $n = 3$ mice per group. Asterisks indicate significant differences at 95% confidence limits. BAL, bronchoalveolar lavage.

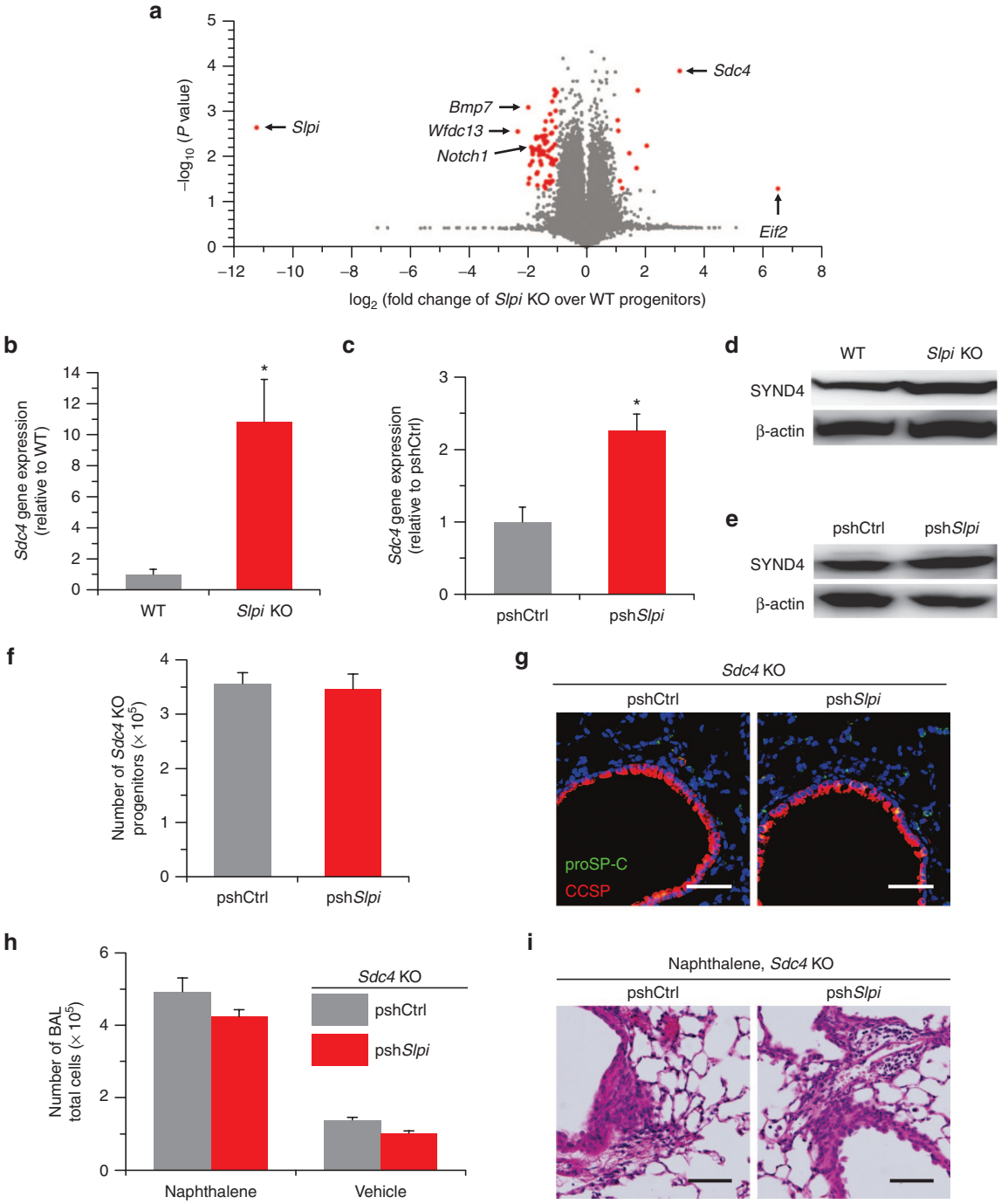

Figure 3 Syndecan 4 is essential to the anti-inflammatory responses induced by impaired secretory leukocyte protease inhibitor expression. (**a**) Volcano plot showing the differential gene expression in microarray analysis between bronchiolar progenitors from *Slpi* KO mice and those from WT mice. Genes that significantly changed more than twofold are indicated in red. *Sdc4*, syndecan 4; *Eif2*, eukaryotic translation initiation factor 2; *Bmp7*, bone morphogenetic protein 7; *Wfdc13*, WAP four-disulfide core domain 13. (**b**,**c**) Quantitative reverse transcription-PCR analysis of syndecan 4 gene expression in bronchiolar progenitors from *Slpi* KO mice (panel **b**) and *Slpi* knockdown mice (panel **c**). Bronchiolar progenitors of WT mice (panel **b**) and pshCtrl-transfected WT mice (panel **c**) were used as a reference. (**d**,**e**) Immunoblotting of syndecan 4 (SYND4) in lung cell lysates of *Slpi* KO mice (panel **d**) and *Slpi* knockdown mice (panel **e**). Controls included lung cells from WT mice (panel **d**) and pshCtrl-transfected WT mice (panel **e**), and β-actin was used as a loading control. For *in vivo* knockdown of the *Slpi* gene (panels **c** and **e**), WT mice were transfected intravenously with 50 µg of psh*Slpi* 48 hours before evaluation. (**f**–**i**) *In vivo* transfection of psh*Slpi* to *Sdc4* KO mice. The study was similar to that in **Figure 2g**–**j**, but *Sdc4* KO mice were transfected intravenously with psh*Slpi* or pshCtrl on day 0. The bronchiolar progenitors in the transfected mice were analyzed by flow cytometry (Lin^{neg} $Sca\text{-}1^{pos}$ AF^{low} cells, panel **f**) and confocal microscopy (scale bar, 50 µm, panel **g**) on day 7. To assess the lung inflammation on day 7, the transfected mice were injected with naphthalene or vehicle on day 1 (panel **h**; scale bar, 100 µm, panel **i**). For panels **b**, **c**, **f**, and **h**, data are reported as the mean ± standard error of $n = 3$ mice per group. Asterisks indicate significant differences at 95% confidence limits. BAL, bronchoalveolar lavage.

transcription-polymerase chain reaction (PCR) analysis of bronchiolar progenitors from *Slpi* KO mice and *in vivo* knockdown mice of the *Slpi* gene (**Figure 3b**,**c**). Bronchiolar progenitors of *Slpi* KO mice expressed 10.8-fold higher amounts of syndecan 4 mRNA than those of WT mice ($P < 0.05$, **Figure 3b**). In WT mice, bronchiolar progenitors had lower syndecan 4 expression than club cells (**Supplementary Figure S10**). After 48 hours of psh*Slpi* injection in WT mice, syndecan 4 mRNA expression was significantly increased in bronchiolar progenitors compared to those of pshCtrl-injected mice ($P < 0.05$, **Figure 3c**). Consistently, immunoblotting of cell lysates revealed greater syndecan 4 expression in total lung cells of *Slpi* KO mice and psh*Slpi*-injected mice, compared to those of WT mice and pshCtrl-injected mice, respectively (**Figure 3d**,**e** and **Supplementary Figure S4b,c**).

To determine whether syndecan 4 contributes to the molecular pathway downstream of decreased SLPI abundance, we analyzed the functional consequences of reduced *Slpi* expression in syndecan 4-deficient (*Sdc4* KO) mice (**Figure 3f**–**i**). Unlike WT mice, *Sdc4* KO mice did not show increased numbers of bronchiolar progenitors defined by the Lin^{neg} $Sca\text{-}1^{pos}$ AF^{low} phenotype in flow cytometry and the CCSP/proSP-C dual positivity in immunofluorescent staining, even after the shRNA-mediated reduction of the SLPI expression ($P > 0.7$, **Figure 3f**,**g** and **Supplementary Figure S6c**). Additionally, we observed that psh*Slpi* injection did not prevent naphthalene-initiated lung inflammation in *Sdc4* KO mice, showing similar inflammatory responses to the pshCtrl injection (naphthalene, psh*Slpi* versus pshCtrl, $P > 0.1$, **Figure 3h**,**i**). These data suggest that syndecan 4, whose expression is negatively regulated by SLPI, is responsible for increasing the number of bronchiolar progenitors that promote the resolution of lung inflammation.

Recombinant syndecan 4 protein has a pharmaceutical value

Given the anti-inflammatory properties of syndecan 4 governing bronchiolar progenitors, together with previous studies suggesting an interaction between syndecan 4 and CXCL10 that inhibits fibroblast recruitment and subsequent lung fibrosis,[25] we focused our functional analyses on the therapeutic potential of recombinant syndecan 4 protein (**Figure 4**). We intravenously treated mice with syndecan 4 (**Figure 4a**–**d**). After 7 days, we found an increase in the number of bronchiolar progenitors by both flow cytometric (Lin^{neg} $Sca\text{-}1^{pos}$ AF^{low} cells) and immunofluorescent staining (CCSP/pro-SP-C dual positive cells) analyses in mice intravenously treated with syndecan 4 as compared to mice treated with the control solvent ($P < 0.05$, **Figure 4a**,**b** and **Supplementary Figure S6d**). The stimulatory effect of syndecan 4 on the number of bronchiolar progenitors was abolished by blockade of the fibroblast growth factor receptor 1 (FGFR1) signaling (PD173074, syndecan 4 versus control, $P > 0.5$, **Supplementary Figure S11**). The increased number of bronchiolar progenitors was also achieved by intratracheal treatment of syndecan 4 ($P < 0.01$, **Supplementary Figure S12**). To evaluate the pharmacological property that reduced bronchiolar inflammation in the lung, we pretreated mice with syndecan 4, followed by intraperitoneal injection of naphthalene into the mice 1 day later (**Figure 4c**,**d**). The pretreatment with syndecan 4 attenuated the naphthalene-induced inflammation in the mice, as judged by a threefold decrease in the number of BAL total cells and reduced cellular infiltration in peribronchial and perivascular tissues, compared to mice pretreated with the control solvent (naphthalene, syndecan 4 versus control, $P < 0.001$, **Figure 4c**,**d**).

To further clarify the effects of therapeutically administered syndecan 4, we intraperitoneally treated WT mice with syndecan 4 six times daily, starting 1 day after intratracheal injection of bleomycin induced alveolar inflammation (**Figure 4e**–**i**). In contrast to mice treated with the control solvent, mice repeatedly treated with syndecan 4 showed reduced inflammation, together with lower numbers of BAL total cells and less mononuclear cell accumulation and thickening in the distal airways and adjacent alveolar spaces (bleomycin, syndecan 4 versus control, $P < 0.005$, **Figure 4e**,**f** and **Supplementary Figure S3d**). Matching the histological features, computed tomography detected extensive, dense consolidation in the lungs of mice treated with the control solvent without syndecan 4 (**Figure 4g**). Concomitant with the diminished inflammation, the therapeutic intervention using syndecan 4 resulted in attenuation of the subsequent fibrotic responses to bleomycin-injured lung; compared to control treatment, the syndecan 4 treatment decreased the amounts of soluble collagen and fibrogenesis-associated proteins, including transforming growth factor β-1 (TGFβ1) and S100-A4 (also known as fibroblast-specific protein-1), in bleomycin-instilled lungs (bleomycin, syndecan 4 versus control, $P < 0.005$, **Figure 4h**,**i** and **Supplementary Figure S4d**). These data support the pharmaceutical potency of syndecan 4 to attenuate various types of lung inflammation and the accompanying fibrotic changes of the lung architecture.

The Nrf2 antioxidant response is integrated with the downstream pathway of syndecan 4

Recently, cellular homeostasis to maintain the airway epithelial health has been shown to be a downstream event in the antioxidant response mediated by Nrf2, which is normally inactivated by interactions with the negative regulator Kelch-like ECH-associated protein 1 (Keap1) in the cytosol.[26,27] Accumulating evidence also indicates that the Keap1-Nrf2 system contributes to lineage-specific differentiation, maintenance and differentiation of stem cells and progenitor cells.[28] We therefore hypothesized that syndecan 4 treatment could modulate the Nrf2 activity to increase the number of bronchiolar progenitors that lead to inflammatory resolution. Seven days after intravenous administration of recombinant syndecan 4 protein in WT mice, immunoblotting of the lung cells revealed that the syndecan 4 treatment decreased the amount of Keap1 protein and increased that of nuclear Nrf2 compared with the control treatment (**Figure 5a** and **Supplementary Figure S4e**). Similar results were achieved in naphthalene- and bleomycin-injured mice (**Supplementary Figure S13**). These results show that syndecan 4 activates the Keap1-Nrf2 pathway by downregulating Keap1, which in turn releases Nrf2 from Keap1 and allows the nuclear accumulation of Nrf2.

To confirm that the nuclear accumulation of Nrf2 by syndecan 4 functions in the antioxidant response, we used *in vivo* models of airway and alveolar inflammation, in which mice were subjected to naphthalene and bleomycin, respectively, 1 day after pretreatment with syndecan 4. After 6 days of rest, we measured

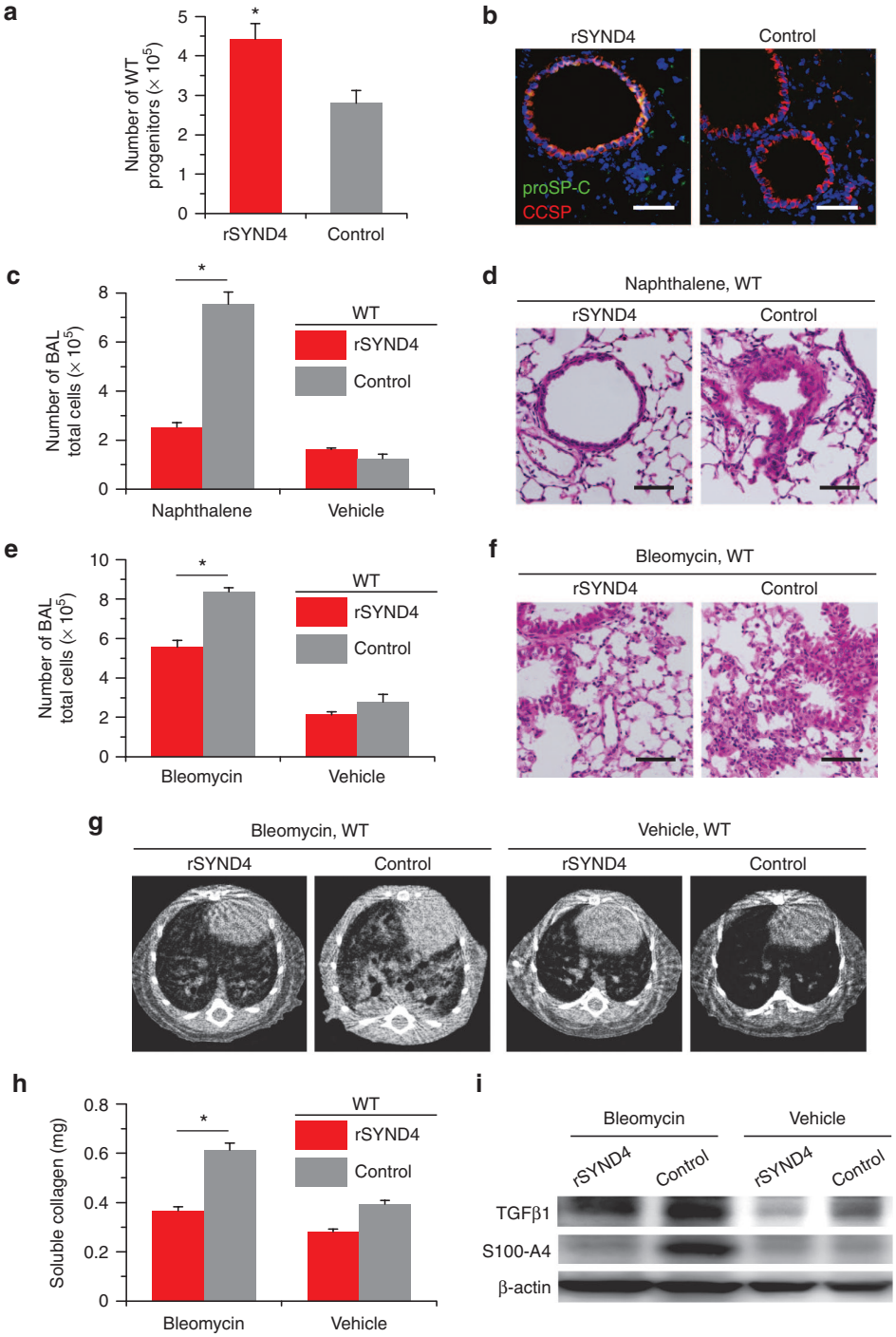

Figure 4 Recombinant syndecan 4 (rSYND4) protein increased the number of bronchiolar progenitors and therapeutically regulated the lung inflammatory responses. (**a**–**d**) Single treatment with syndecan 4. The study was similar to that in **Figure 2a**–**d**, but WT mice were treated intravenously with 20 µg syndecan 4 or the solvent (control) on day 0. The bronchiolar progenitors in the treated mice were analyzed by flow cytometry (Lin^{neg} $Sca\text{-}1^{pos}$ AF^{low} cells, panel **a**) and confocal microscopy (scale bar, 50 µm, panel **b**) on day 7. To assess the lung inflammation on day 7, the treated mice were injected with naphthalene or vehicle on day 1 (panel **c**; scale bar, 100 µm, panel **d**). (**e**–**i**) Repeated treatment of bleomycin-induced inflammation with syndecan 4. WT mice were injected intratracheally with bleomycin or vehicle (day 1). On days 2–7, the injected mice were treated daily with intraperitoneal administration of 4 µg syndecan 4 or the solvent (control). On day 8, the lung inflammation was assessed by total counts of cells in the BAL fluid (panel **e**), histological examination of the lung sections stained with H&E (scale bar, 100 µm, panel **f**), computed tomographic examination of the lungs (panel **g**), soluble collagen levels in the right lungs (panel **h**), and immunoblotting of TGFβ1 and S100-A4 in lung cell lysates (β-actin, loading control, panel **i**). For panels **a**, **c**, **e**, and **h**, data are reported as the mean ± standard error of $n = 3$ mice per group. Asterisks indicate significant differences at 95% confidence limits. BAL, bronchoalveolar lavage; H&E, hematoxylin and eosin.

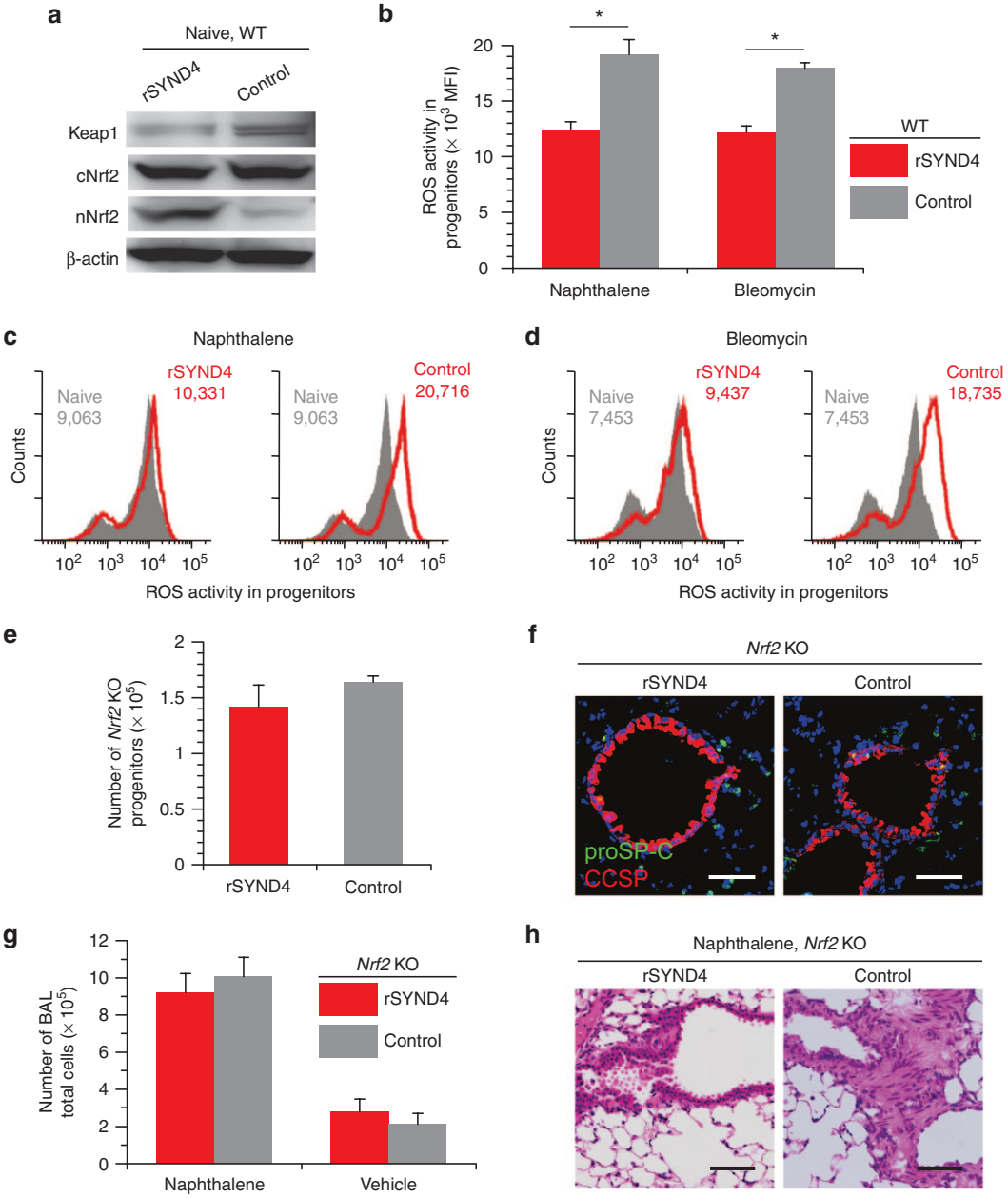

Figure 5 Syndecan 4 suppressed reactive oxygen species (ROS) production in bronchiolar progenitors, increasing their numbers and decreasing the lung inflammation via nuclear translocation of Nrf2. (**a**) Immunoblotting of Keap1, and cytoplasmic and nuclear fractions of Nrf2 (cNrf2 and nNrf2, respectively). (**b**–**d**) ROS in bronchiolar progenitors, which were quantified (panel **b**) and visualized (panels **c** and **d**). For panels **a**–**d**, WT mice were treated intravenously with 20 µg syndecan 4 or the solvent (control) on day 0. For panel **a**, on day 7, the lung cells were subjected to the analysis, and β-actin was used as a loading control. For panels **b**–**d**, the treated mice were injected with naphthalene intraperitoneally (panels **b** and **c**) or bleomycin intratracheally (panels **b** and **d**) on day 1, and lung cells were stained with a H_2DCFDA derivative to determine the intracellular ROS level of bronchiolar progenitors in Lin^{neg} Sca-1^{pos} AF^{low} fraction as the mean fluorescent intensity (MFI) of flow cytometry on day 7. For panels **c** and **d**, the gray histogram overlaid in each panel depicts bronchiolar progenitors from sham-controlled mice (naive), and the MFI of stained cells are shown in each panel. (**e**–**h**) Treatment of *Nrf2* KO mice with syndecan 4. The study was similar to that in **Figure 4a**–**d**, but *Nrf2* KO mice were treated intravenously with syndecan 4 or the solvent (control) on day 0. The bronchiolar progenitors in the treated mice were analyzed by flow cytometry (Lin^{neg} Sca-1^{pos} AF^{low} cells, panel **e**) and confocal microscopy (scale bar, 50 µm, panel **f**) on day 7. To assess the lung inflammation on day 7, the treated mice were injected with naphthalene or vehicle on day 1 (panel **g**; scale bar, 100 µm, panel **h**). For panels **b**, **e**, and **g**, data are reported as the mean ± standard error of $n = 3$ mice per group. Asterisks indicate significant differences at 95% confidence limits. BAL, bronchoalveolar lavage.

the reactive oxygen species (ROS) activity in Lin^{neg} Sca-1^{pos} AF^{low} bronchiolar progenitors by flow cytometry using a ROS-sensitive fluorescent probe (**Figure 5b**–**d**). Bronchiolar progenitors from naphthalene-injected mice showed a significant decrease in the ROS levels upon syndecan 4 pretreatment as compared with control pretreatment, and the ROS level of mice pretreated with syndecan 4 was comparable to that of naive mice (naphthalene, syndecan 4 versus control, $P < 0.05$, **Figure 5b,c**). We observed essentially similar results in bronchiolar progenitors isolated from bleomycin-injected mice (bleomycin, syndecan 4 versus control,

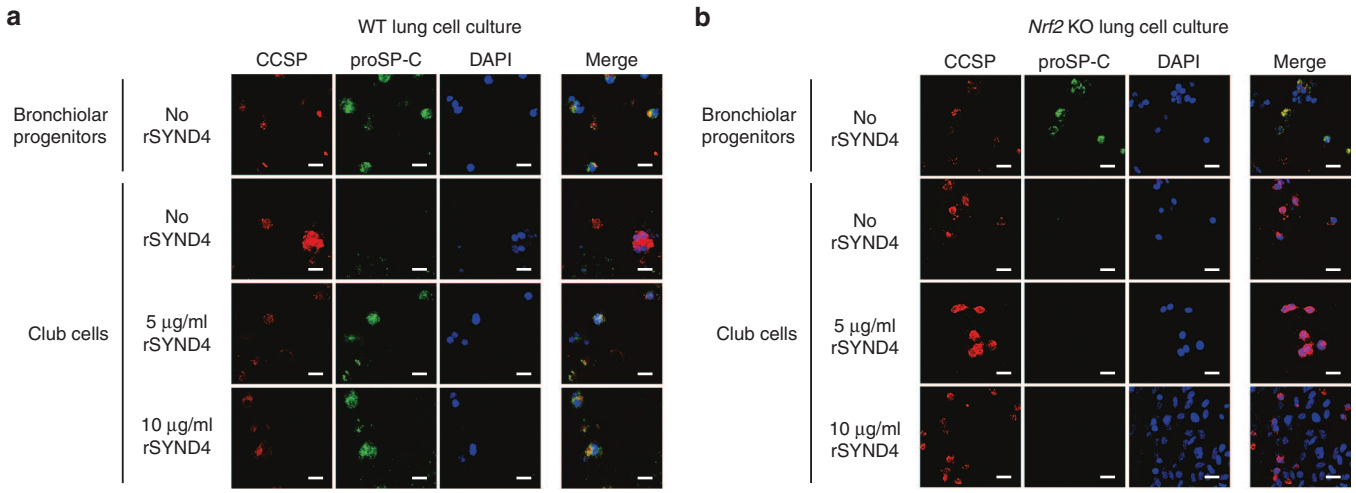

Figure 6 ***In vitro*** **3D culture for differentiation of club cells to bronchiolar progenitors.** Bronchiolar progenitor (Lin^{neg} Sca-1^{pos} AF^{low}) and club cell (Lin^{neg} Sca-1^{pos} AF^{high}) fractions were sorted from lung cells of WT mice (panel **a**) and *Nrf2* KO mice (panel **b**) by flow cytometry. Each cell fraction was seeded at a density of 1.3×10^3 cells in 100 µl of 50% Matrigel in a 24-well transwell insert together with 10^5 MLg cells, a mouse lung fibroblast cell line. The Matrigel was cultured in the presence (5 or 10 µg/ml) or absence of syndecan 4. After 7 days, the cultures were stained for acquiring fluorescent confocal images of CCSP (red), proSP-C (green), DAPI (nuclei, blue), and their overlay (merge). Scale bar, 20 µm. DAPI, 4′,6-diamidino-2-phenylindole, dihydrochloride.

$P < 0.005$, **Figure 5b,d**), clearly showing that syndecan 4 activates the Keap1-Nrf2 pathway, which serves to eliminate the oxidative stress from bronchiolar progenitors.

We next tested whether the Keap1-Nrf2 pathway is fundamentally linked to the pharmaceutical mechanisms by which syndecan 4 increases the number of bronchiolar progenitors and dampens lung inflammation (**Figure 5e–h**). To address this, we treated *Nrf2*-deficient (*Nrf2* KO) mice with intravenous injection of recombinant syndecan 4 protein. In contrast to WT mice (**Figure 4a,b**), *Nrf2* KO mice treated with syndecan 4 and the control solvent showed comparable numbers of bronchiolar progenitors that were defined as the Lin^{neg} Sca-1^{pos} AF^{low} phenotype in flow cytometry and the CCSP/proSP-C dual positivity in immunostaining ($P > 0.3$, **Figure 5e,f** and **Supplementary Figure S6e**). We made corresponding observations in *Nrf2* KO mice that had been subjected to naphthalene-induced lung inflammation after pretreatment with syndecan 4 (**Figure 5g,h**). The genetic ablation of Nrf2 abrogated the syndecan 4-mediated beneficial responses to the inflammation, with no differences in BAL total cells and histological features between syndecan 4 and control pretreatments (naphthalene, syndecan 4 versus control, $P > 0.2$, **Figure 5g,h**). There was no significant difference between WT and *Nrf2* KO mice in number of total BAL cells under naive condition ($P > 0.6$, **Supplementary Figure S14**). Collectively, these data suggest that the Keap1-Nrf2 pathway is essential for syndecan 4 to elicit the anti-inflammatory effects associated with increased numbers of bronchiolar progenitors.

Syndecan 4 evokes Nrf2-dependent transition from club cells to bronchiolar progenitors

There is accumulating evidence that diverse somatic cells are highly plastic and can transition from one type to another, suggesting that dedifferentiation might be a potential mechanism to increase the number of bronchiolar progenitors *in vivo* in response to syndecan 4 through the Nrf2-dependent pathway.[9,29] To test this hypothesis, we isolated Lin^{neg} Sca-1^{pos} AF^{high} club cells from WT or *Nrf2* KO mice by flow cytometry, placed them in 3D culture for 7 days with syndecan 4, and examined the cellular state by immunofluorescent staining of CCSP and proSP-C (**Figure 6**). The results of immunostaining showed that syndecan 4 treatment of the club cells from WT mice promoted the expression of proSP-C, rather than the CCSP that was favored in the untreated control club cells; there was no difference between lower and higher doses of syndecan 4 with respect to the appearance of CCSP/proSP-C dual positive cells, which were also observed in untreated bronchiolar progenitors (**Figure 6a**). Neither expression of cytokeratin 5 (basal cell marker) nor LAMP3 (alveolar type 2 cell marker) was detected in bronchiolar progenitors as well as club cells treated with or without syndecan 4 (**Supplementary Figure S15**). In contrast, club cells from the *Nrf2* KO mice were compromised to induce proSP-C expression, even after they had been treated with either lower or higher doses of syndecan 4, although bronchiolar progenitors from the *Nrf2* KO mice showed comparable staining for CCSP and proSP-C to those from WT mice (**Figure 6b**). Thus, syndecan 4 promoted the transition of club cells to bronchiolar progenitors through the activation of Nrf2-dependent pathway, which increased the number of anti-inflammatory bronchiolar progenitors after the systemic administration of syndecan 4 *in vivo*.

DISCUSSION

Our goal in this study was to delineate the cellular and molecular mechanisms by which club cells and/or the multipotent subset of club cells known as bronchiolar progenitors develop anti-inflammatory responses in lung. When adoptively transferred into mice, bronchiolar progenitors, but not club cells, reduced naphthalene-induced lung inflammation. Notably, in an attempt to further characterize the bronchiolar progenitors, we found that there were significantly more bronchiolar progenitors in the small airways of *Slpi* KO mice than in those of WT mice. Using microarray analysis of the bronchiolar progenitors, we identified a marked upregulation of syndecan 4 in bronchiolar progenitors from *Slpi* KO mice

as compared to those from WT mice. Our *in vivo* data in the two mouse models of inflammatory lung disease showed that recombinant syndecan 4 increased the number of bronchiolar progenitors providing a therapeutic effect on lung inflammation. Our *in vitro* data of Matrigel 3D cultures also showed that the functional attributes of syndecan 4 are due to stimulating the Nrf2-dependent transition from club cells to bronchiolar progenitors.

Club cells, indistinguishable from bronchiolar progenitors, were first described in the late 19th century.[17] By virtue of exquisite studies made since, several lung-protective aspects have been demonstrated in these cells.[16,17] The physiologic roles have been mainly ascribed in pulmonary biology to their secretory proteins, because the presence of secretory granules was recognized in the initial description and have been used for morphologic identification of the cells.[16,17,30–32] The proteins that are known to be secreted include CCSP, SLPI, club cell 55-kDa protein, surfactant proteins, club cell tryptase, and β-galactoside-binding lectin.[16,17] Especially, much attention has been paid to CCSP, which was identified as the dominant secretory protein, and early data from mice deficient in CCSP suggested that club cells resolved lung inflammation directly owing to CCSP per se.[33,34] However, CCSP deficiency alters not only the CCSP expression but also the protein composition of the fluid lining the airway.[35] This evidence suggests that lung epithelial homeostasis, which could be disturbed in CCSP-deficient mice, is also implicated in the protective machinery against lung inflammation.

In this context, our adoptive transfer experiment using sorted cells demonstrated that bronchiolar progenitors with lower CCSP levels, but not club cells with higher CCSP levels, could attenuate airway inflammation that developed after naphthalene-induced club cell depletion in a species-selective manner. The similar attenuation associated with bronchiolar progenitors was also achieved in another inflammation model using a more common pulmonary toxicant, bleomycin. The bronchiolar progenitors sorted for the Lin^{neg} Sca-1^{pos} AF^{low} phenotype showed higher expression levels of proSP-C, SP-D, and SLPI. While the small molecular weight hydrophobic surfactant protein SP-C is involved in surface tension regulatory functions, the large hydrophilic surfactant protein SP-D maintains an inflammation-free lung by promoting homeostatic clearance of apoptotic cells, inhibiting the release of pro-inflammatory cytokines, and directly modulating the cellular functions of macrophages, dendritic cells, and T cells.[19] We and others have also identified anti-inflammatory effects of SLPI, which attenuates nuclear factor (NF)-κB-dependent inflammatory responses by stabilizing interleukin-1 receptor-associated kinase (IRAK), IκBα, and IκBβ proteins.[18,36–39] Further, the Lin^{neg} Sca-1^{pos} AF^{low} fraction, which preferentially includes bronchiolar progenitors, has been reported to harbor a mixed population.[14] Thus, secretory factors other than CCSP (*e.g.*, SP-D and SLPI) may be also required for the functional capacity of bronchiolar progenitors to control inflammatory conditions.

Not only did this study demonstrate higher SLPI levels in bronchiolar progenitors than in club cells, but also clarified a molecular pathway downstream of SLPI. We showed that impaired SLPI expression in both *Slpi* KO mice and *in vivo Slpi* knockdown mice increased syndecan 4 expression by bronchiolar progenitors. Hence, we identified a SLPI-mediated negative regulation of syndecan 4, which encourages cellular transition from club cells to bronchiolar progenitors, as evidenced by our 3D findings in the *in vitro* culture. We therefore considered that the relationship between club cells and bronchiolar progenitors could be maintained through equilibrium feedback loops that involve SLPI and syndecan 4; SLPI in bronchiolar progenitors represses the expression of syndecan 4, a potent inducer of bronchiolar progenitors, allowing them to differentiate toward club cells, whereas club cells lose the SLPI expression and thereby enhance their tendency to dedifferentiate toward bronchiolar progenitors (**Supplementary Figure S16**). This notion is also supported by our results showing that the *in vivo Slpi* knockdown using shRNA increased the number of bronchiolar progenitors in WT mice, but not in *Sdc4* KO mice.

This phenotypic plasticity of club cells even in a differentiated state is consistent with previous observations showing that a majority of CCSP-positive cells in bronchioles, including bronchiolar progenitors and club cells, have the potential for self-renewal and transition to another cell type.[40] The underlying concept is that differentiated club cells go through a process of dedifferentiation to bronchiolar progenitors in order to re-enter the cell cycle for their self-renewal before redifferentiating to either club cells or ciliated cells. Similar plasticity in the differentiative potential is also found in alveolar type 2 cells, which reveal differentiated functions in the biosynthesis of pulmonary surfactant while retaining their capacity for self-renewal and differentiation into alveolar type 1 cells.[41,42] Such plasticity of differentiated somatic cells is not unique to the lung, and many studies have expanded to analyze the process by which diverse cell types dedifferentiate to become less specialized, multipotent cells in various types of tissues.[9,29,43] Although epigenetic reprogramming through covalent modifications on chromatin is generally thought to contribute to the dedifferentiation process, the precise molecular steps involved in the lung cell dedifferentiation are not yet fully understood.[5,7–9,44] Further understanding of the pathways that support bronchiolar progenitor homeostasis could enable novel therapeutic approaches in inflammatory lung diseases.

MATERIALS AND METHODS

Mice. *Slpi*-deficient (*Slpi* KO), syndecan 4-deficient (*Sdc4* KO), and *Nrf2*-deficient (*Nrf2* KO) mice were generated as described previously and had been backcrossed to C57BL/6 mice.[38,45,46] There were no differences of leukocyte composition in peripheral blood among these mice (**Supplementary Figure S17**). All procedures were performed according to protocols approved by Tohoku University's Institutional Committee for the Use and Care of Laboratory Animals.

Naphthalene- or bleomycin-initiated lung inflammation. Mice were intraperitoneally injected with naphthalene (Sigma-Aldrich, St. Louis, MO), or intratracheally with bleomycin hydrochloride (Nippon Kayaku, Tokyo, Japan). Six or 7 days later, BAL was performed and lung tissues were collected for histopathological analysis as described previously.[47,48] Additional details on the method for these measurements is provided in **Supplementary Materials and Methods**.

Statistical analysis. Statistical comparison was made using Student's unpaired two-tailed *t*-test. *P* values less than 0.05 were considered statistically significant.

SUPPLEMENTARY MATERIAL

Figure S1. Cytoplasmic/nucleus ratios of club cells and bronchiolar progenitors shown in **Figure. 1a.**

Figure S2. Tissue macrophages in lungs after BAL.

Figure S3. Elastica-Masson staining.

Figure S4. Quantification of the protein expression.

Figure S5. In vivo transfection of a plasmid vector expressing *Slpi* (p*Slpi*) in *Slpi* KO mice.

Figure S6. Separate photomicrographs of merged images shown in **Figure 2b** (**S6a**), **Figure 2h** (**S6b**), **Figure 3g** (**S6c**), **Figure 4b** (**S6d**), and **Figure 5f** (**S6e**).

Figure S7. Total and differential counts of cells recovered in the BAL fluid.

Figure S8. Lung inflammation via repeated administration of naphthalene in *Slpi* KO mice.

Figure S9. No detectable differences in the numbers of Sca-1-positive cells outside the bronchiolar epithelium and CD31-positive cells between wild-type (WT) and *Slpi*-deficient mice (*Slpi* KO), or between pshCtrl- and psh*Slpi*-transfected wild-type mice.

Figure S10. Syndecan 4 expression analysis by western blot in bronchiolar progenitors and club cells from WT mice.

Figure S11. Recombinant syndecan 4 (rSYND4) protein did not increase the number of bronchiolar progenitors in blockade of the FGFR1 signaling.

Figure S12. Recombinant syndecan 4 (rSYND4) protein increased the number of bronchiolar progenitors, even when injected by the intratracheal route.

Figure S13. Immunoblotting of Nrf2 in syndecan 4-treated mice after injury.

Figure S14. The cellular aspect of BAL from *Nrf2* KO mice in the naive condition.

Figure S15. Cytokeratin 5 and LAMP3 staining.

Figure S16. Schematic of our model.

Figure S17. Leukocyte composition of mice used in this study.

Table S1. Upregulated 10 genes in bronchiolar progenitors of *Slpi* KO mice compared to those of WT mice.

Table S2. Downregulated 61 genes in bronchiolar progenitors of *Slpi* KO mice compared to those of WT mice.

Materials and Methods

ACKNOWLEDGMENTS

We thank Mitsu Takahashi for her technical assistance. These studies were supported, in part, by Grants-in-Aid for Scientific Research from the Ministry of Education, Culture, Sports, Science and Technology (No. 23390219 and No. 15K15316, Tokyo, Japan), and the Core Research for Evolutional Science and Technology Program from the Japan Science and Technology Agency (Tokyo, Japan). The authors have no financial relationships relevant to this manuscript to disclose.

REFERENCES

1. Kotton, DN (2012). Next-generation regeneration: the hope and hype of lung stem cell research. *Am J Respir Crit Care Med* **185**: 1255–1260.
2. Lau, AN, Goodwin, M, Kim, CF and Weiss, DJ (2012). Stem cells and regenerative medicine in lung biology and diseases. *Mol Ther* **20**: 1116–1130.
3. Rackley, CR and Stripp, BR (2012). Building and maintaining the epithelium of the lung. *J Clin Invest* **122**: 2724–2730.
4. Rock, J and Königshoff, M (2012). Endogenous lung regeneration: potential and limitations. *Am J Respir Crit Care Med* **186**: 1213–1219.
5. Ardhanareeswaran, K and Mirotsou, M (2013). Lung stem and progenitor cells. *Respiration* **85**: 89–95.
6. Bertoncello, I and McQualter, JL (2013). Lung stem cells: do they exist? *Respirology* **18**: 587–595.
7. Green, MD, Huang, SX and Snoeck, HW (2013). Stem cells of the respiratory system: from identification to differentiation into functional epithelium. *Bioessays* **35**: 261–270.
8. Herriges, M and Morrisey, EE (2014). Lung development: orchestrating the generation and regeneration of a complex organ. *Development* **141**: 502–513.
9. Hogan, BL, Barkauskas, CE, Chapman, HA, Epstein, JA, Jain, R, Hsia, CC *et al.* (2014). Repair and regeneration of the respiratory system: complexity, plasticity, and mechanisms of lung stem cell function. *Cell Stem Cell* **15**: 123–138.
10. Ryu, JH, Myers, JL and Swensen, SJ (2003). Bronchiolar disorders. *Am J Respir Crit Care Med* **168**: 1277–1292.
11. Hong, KU, Reynolds, SD, Giangreco, A, Hurley, CM and Stripp, BR (2001). Clara cell secretory protein-expressing cells of the airway neuroepithelial body microenvironment include a label-retaining subset and are critical for epithelial renewal after progenitor cell depletion. *Am J Respir Cell Mol Biol* **24**: 671–681.
12. Giangreco, A, Reynolds, SD and Stripp, BR (2002). Terminal bronchioles harbor a unique airway stem cell population that localizes to the bronchoalveolar duct junction. *Am J Pathol* **161**: 173–182.
13. Teisanu, RM, Lagasse, E, Whitesides, JF and Stripp, BR (2009). Prospective isolation of bronchiolar stem cells based upon immunophenotypic and autofluorescence characteristics. *Stem Cells* **27**: 612–622.
14. Teisanu, RM, Chen, H, Matsumoto, K, McQualter, JL, Potts, E, Foster, WM *et al.* (2011). Functional analysis of two distinct bronchiolar progenitors during lung injury and repair. *Am J Respir Cell Mol Biol* **44**: 794–803.
15. Guha, A, Vasconcelos, M, Cai, Y, Yoneda, M, Hinds, A, Qian, J *et al.* (2012). Neuroepithelial body microenvironment is a niche for a distinct subset of Clara-like precursors in the developing airways. *Proc Natl Acad Sci USA* **109**: 12592–12597.
16. Reynolds, SD and Malkinson, AM (2010). Clara cell: progenitor for the bronchiolar epithelium. *Int J Biochem Cell Biol* **42**: 1–4.
17. Singh, G and Katyal, SL (2000). Clara cell proteins. *Ann N Y Acad Sci* **923**: 43–58.
18. Wilkinson, TS, Roghanian, A, Simpson, AJ and Sallenave, JM (2011). WAP domain proteins as modulators of mucosal immunity. *Biochem Soc Trans* **39**: 1409–1415.
19. Orgeig, S, Hiemstra, PS, Veldhuizen, EJ, Casals, C, Clark, HW, Haczku, A *et al.* (2010). Recent advances in alveolar biology: evolution and function of alveolar proteins. *Respir Physiol Neurobiol* **173 Suppl**: S43–S54.
20. Klimenkova, O, Ellerbeck, W, Klimiankou, M, Ünalan, M, Kandabarau, S, Gigina, A *et al.* (2014). A lack of secretory leukocyte protease inhibitor (SLPI) causes defects in granulocytic differentiation. *Blood* **123**: 1239–1249.
21. van 't Wout, EF, Hiemstra, PS and Marciniak, SJ (2014). The integrated stress response in lung disease. *Am J Respir Cell Mol Biol* **50**: 1005–1009.
22. Mou, H, Zhao, R, Sherwood, R, Ahfeldt, T, Lapey, A, Wain, J *et al.* (2012). Generation of multipotent lung and airway progenitors from mouse ESCs and patient-specific cystic fibrosis iPSCs. *Cell Stem Cell* **10**: 385–397.
23. Hagiwara, K, Kikuchi, T, Endo, Y, Huqun, Usui, K, Takahashi, M *et al.* (2003). Mouse SWAM1 and SWAM2 are antibacterial proteins composed of a single whey acidic protein motif. *J Immunol* **170**: 1973–1979.
24. Xing, Y, Li, A, Borok, Z, Li, C and Minoo, P (2012). NOTCH1 is required for regeneration of Clara cells during repair of airway injury. *Stem Cells* **30**: 946–955.
25. Jiang, D, Liang, J, Campanella, GS, Guo, R, Yu, S, Xie, T *et al.* (2010). Inhibition of pulmonary fibrosis in mice by CXCL10 requires glycosaminoglycan binding and syndecan-4. *J Clin Invest* **120**: 2049–2057.
26. Holmström, KM and Finkel, T (2014). Cellular mechanisms and physiological consequences of redox-dependent signalling. *Nat Rev Mol Cell Biol* **15**: 411–421.
27. Paul, MK, Bisht, B, Darmawan, DO, Chiou, R, Ha, VL, Wallace, WD *et al.* (2014). Dynamic changes in intracellular ROS levels regulate airway basal stem cell homeostasis through Nrf2-dependent Notch signaling. *Cell Stem Cell* **15**: 199–214.
28. Murakami, S and Motohashi, H (2015). Roles of NRF2 in cell proliferation and differentiation. *Free Radic Biol Med* (in press).
29. Blanpain, C and Fuchs, E (2014). Stem cell plasticity. Plasticity of epithelial stem cells in tissue regeneration. *Science* **344**: 1242281.
30. Singh, G, Katyal, SL, Ward, JM, Gottron, SA, Wong-Chong, ML and Riley, EJ (1985). Secretory proteins of the lung in rodents: immunocytochemistry. *J Histochem Cytochem* **33**: 564–568.
31. Singh, G and Katyal, SL (1984). An immunologic study of the secretory products of rat Clara cells. *J Histochem Cytochem* **32**: 49–54.
32. Patton, SE, Gilmore, LB, Jetten, AM, Nettesheim, P and Hook, GE (1986). Biosynthesis and release of proteins by isolated pulmonary Clara cells. *Exp Lung Res* **11**: 277–294.
33. Broeckaert, F, Clippe, A, Knoops, B, Hermans, C and Bernard, A (2000). Clara cell secretory protein (CC16): features as a peripheral lung biomarker. *Ann N Y Acad Sci* **923**: 68–77.
34. Stripp, BR, Reynolds, SD, Plopper, CG, Bøe, IM and Lund, J (2000). Pulmonary phenotype of CCSP/UG deficient mice: a consequence of CCSP deficiency or altered Clara cell function? *Ann N Y Acad Sci* **923**: 202–209.
35. Stripp, BR, Reynolds, SD, Boe, IM, Lund, J, Power, JH, Coppens, JT *et al.* (2002). Clara cell secretory protein deficiency alters clara cell secretory apparatus and the protein composition of airway lining fluid. *Am J Respir Cell Mol Biol* **27**: 170–178.
36. Jin, FY, Nathan, C, Radzioch, D and Ding, A (1997). Secretory leukocyte protease inhibitor: a macrophage product induced by and antagonistic to bacterial lipopolysaccharide. *Cell* **88**: 417–426.
37. Lentsch, AB, Jordan, JA, Czermak, BJ, Diehl, KM, Younkin, EM, Sarma, V *et al.* (1999). Inhibition of NF-kappaB activation and augmentation of IkappaBbeta by secretory leukocyte protease inhibitor during lung inflammation. *Am J Pathol* **154**: 239–247.
38. Nakamura, A, Mori, Y, Hagiwara, K, Suzuki, T, Sakakibara, T, Kikuchi, T *et al.* (2003). Increased susceptibility to LPS-induced endotoxin shock in secretory leukoprotease inhibitor (SLPI)-deficient mice. *J Exp Med* **197**: 669–674.
39. Taggart, CC, Greene, CM, McElvaney, NG and O'Neill, S (2002). Secretory leucoprotease inhibitor prevents lipopolysaccharide-induced IkappaBalpha degradation without affecting phosphorylation or ubiquitination. *J Biol Chem* **277**: 33648–33653.
40. Rawlins, EL, Okubo, T, Xue, Y, Brass, DM, Auten, RL, Hasegawa, H *et al.* (2009). The role of Scgb1a1+ Clara cells in the long-term maintenance and repair of lung airway, but not alveolar, epithelium. *Cell Stem Cell* **4**: 525–534.
41. Barkauskas, CE, Cronce, MJ, Rackley, CR, Bowie, EJ, Keene, DR, Stripp, BR *et al.* (2013). Type 2 alveolar cells are stem cells in adult lung. *J Clin Invest* **123**: 3025–3036.
42. Desai, TJ, Brownfield, DG and Krasnow, MA (2014). Alveolar progenitor and stem cells in lung development, renewal and cancer. *Nature* **507**: 190–194.
43. Fuhrmann, S, Zou, C and Levine, EM (2014). Retinal pigment epithelium development, plasticity, and tissue homeostasis. *Exp Eye Res* **123**: 141–150.

44. Apostolou, E and Hochedlinger, K (2013). Chromatin dynamics during cellular reprogramming. *Nature* **502**: 462–471.
45. Ishiguro, K, Kadomatsu, K, Kojima, T, Muramatsu, H, Tsuzuki, S, Nakamura, E *et al.* (2000). Syndecan-4 deficiency impairs focal adhesion formation only under restricted conditions. *J Biol Chem* **275**: 5249–5252.
46. Itoh, K, Chiba, T, Takahashi, S, Ishii, T, Igarashi, K, Katoh, Y *et al.* (1997). An Nrf2/small Maf heterodimer mediates the induction of phase II detoxifying enzyme genes through antioxidant response elements. *Biochem Biophys Res Commun* **236**: 313–322.
47. Daito, H, Kikuchi, T, Sakakibara, T, Gomi, K, Damayanti, T, Zaini, J *et al.* (2011). Mycobacterial hypersensitivity pneumonitis requires TLR9-MyD88 in lung CD11b+ CD11c+ cells. *Eur Respir J* **38**: 688–701.
48. Damayanti, T, Kikuchi, T, Zaini, J, Daito, H, Kanehira, M, Kohu, K *et al.* (2010). Serial OX40 engagement on CD4+ T cells and natural killer T cells causes allergic airway inflammation. *Am J Respir Crit Care Med* **181**: 688–698.